Deep-salt: complete 3D salt segmentation from inaccurate migrated subsurface offset gathers using deep learning

Ana Paula O. Muller [1 2] *, Bernardo M. O. Fraga [2], Jessé C. Costa [3 4], Clecio R. Bom [2 5], Matheus Klatt [2], Elisangela L. Faria [2], Marcelo P. de Albuquerque [2], Marcio P. de Albuquerque [2]
1) Petróleo Brasileiro S.A. (PETROBRAS), 2) Centro Brasileiro de Pesquisas Físicas (CBPF), 3) Universidade Federal do Pará (UFPA), 4) Institute of Petroleum Geophysics (INCT-GP), 5) Centro Federal de Educação Tecnológica Celso Suckow da Fonseca (CEFET-RJ)

This paper was prepared for presentation during the 18th International Congress of the Brazilian Geophysical Society held in Rio de Janeiro, Brazil, 16-19 October 2023.

Abstract

Delimiting salt inclusions from migrated images during the velocity model building flow is a time-consuming activity that depends on highly human-curated analysis and is subject to interpretation errors or limitations of the images and methods available. This work proposes a supervised Deep Learning (DL) based method to include 3D salt geometries in the velocity models. The proposed methodology is based on using the subsurface offset gathers as the input to a U-Net which is trained to predict the correct salt inclusions, which was previously validated for 2D approaches. We generated the subsurface offset gathers using RTM (Reverse Time Migration) with an extended imaging condition. The velocity model used in migration is inaccurate (with a reasonable approximation of sediment velocity but without salt inclusions). We trained a U-Net to use common-offset subsurface gathers as input channels and the correct salt masks as the output of a supervised semantic segmentation problem. Our approach relies on subsurface common image gathers to focus the sediments' reflections around the zero offset and to spread the energy of salt reflections over large subsurface offsets. The training process tuned the U-Net to successfully learn the shape of complex salt body masks with high accuracy from partially focused subsurface offset images. Moreover, it also performed well when applied to synthetic benchmark data-set that were not previously introduced in network training.

Introduction

Velocity model building (VMB) is essential to make accurate subsurface images, especially in regions with high contrast and structurally complex velocities. One good example of the limitation of conventional inverse methods is the inclusion of salt bodies in the velocity model, a complex non-automated method that poses a high cost and is subject to uncertainties. Salt inclusion is critical during the VMB. Hence a mistake in the salt's geometry makes the image below the salt unfocused or distorted [1], generating a wrong structure of the subsurface. Therefore, it can lead to economic consequences, especially in petroleum provinces where the reservoirs are below complex salt structures. Salt presents a great diversity of possible geometries and has a high-velocity contrast with the enclosing sediments. In complex areas, the definition of the salt geometry is estimated in an iterative process called salt flood which requires massive human interpretation input, geological knowledge of the sedimentary basin, and testing of different scenarios.

Many recent works are using DL to obtain the velocity models[2], being particularly successful in predicting the salt bodies embedded in such models from raw shot data [3], even those with very complex geometries. The initial approaches, e.g. [4], used the raw seismic shot data to train the network to fully predict the correct velocity model that generated those seismic shots. Their results are very encouraging; however, they can not be easily extended to current seismic field data. The size of real seismic acquisitions is much larger than the most modern device could support, and even if they could be supported, the number of convolution operations would be prohibitive. Besides, there is the irregularity of seismic shots and the geometric non-correspondence of this data with the seismic images or the velocity models.

One alternative to reduce the data size and the complexity of the task is to address the DL method only for the task of salt inclusions, by the use of migrated images [5] or FWI gradient responses [6]. Salt prediction proposed in [5], reduces the input data to the imaging domain, by migrating the shots with a reasonable sediment velocity model, without any salt inclusions. Then the neural network was trained to return only the salt inclusions. This flow defines a hybrid approach of the conventional VMB workflow and DL velocity estimation from seismic data, using DL only in the most challenging step of VMB flow: the inclusion of salt structures.

Despite the successful results, previous salt inclusion guided by DL relied on 2D simulations and 2D DL architectures. The extension to 3D simulations requires careful DL design to avoid memory issues on the GPUs. In this work, we propose to extend the salt segmentation methodology proposed in [5] to 3D data, using as DL architecture a U-Net with support for 3D cubes. We tested

this approach over a synthetic seismic data set and showed that the DL model could segment 3D salt geometries.

Methods

We migrated the shot seismic data using RTM (Reverse Time Migration) with cross-correlation extended imaging condition [7], which for the 3D case can be written as

$$I(x,\ y,\ z,\ \lambda_x,\ \lambda_y) = \sum_{shots} \sum_{t} [W_s(x - \lambda_x, y - \lambda_y, z, t)\ X\ W_r(x + \lambda_x, y + \lambda_y, z, t)] \quad (1)$$

Considering that usually salt inclusion is made in a stage of velocity model building flow when the sediment velocity is well-resolved, the shots are migrated with a reasonable sediment velocity model, without any salt inclusions. Since we are working with synthetic data, this velocity model is generated by a smoothed version of the sediment velocity. For each investigated subsurface offset (λ_x or λ_y), a different image is generated.

Subsurface offsets have one interesting property that differs from the well-known surface offset, which was decisive in choosing this representation for the salt segmentation method. An event migrated with its correct velocity model, concentrates the reflections' energy in $\lambda_x = \lambda_y = 0$, while the uncorrected migrated events spread their energy over the far offsets. It is expected that the predominant events observed in high subsurface offsets to be associated with the salt reflections. To migrate the subsurface offset panels, we varied λ_x and λ_y independently, creating fifteen panels to be used as input for the neural network training, with the minimum value equal to zero, and the maximum value for λ_x = 250m and for $\lambda_y = 312.5$m. The maximum subsurface offsets were empirically chosen in order to capture the maximum offset where it was possible to observe coherent events.

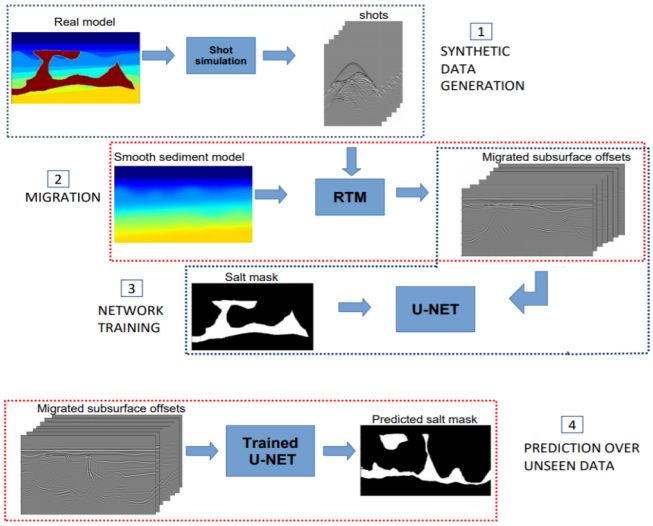

Figure 1: Summary of the salt prediction pipeline as proposed for 2D in [5] .

The supervised learning pipeline proposed for 2D models in [5] is summarized in Figure 1. The inputs are the cubes of migrated subsurface offsets, with each value of subsurface offset corresponding to one channel of the input image. The outputs are the cubes with the segmented salt geometry.

Our training/validation/test set consists of 30 synthetic velocity models with full coverage acquisition region equal to 2 km of depth, 4 km of extension in the inline direction, and 3 km in the crossline direction The spatial sampling rate is equal to 12.5 m for the three directions. We linearly extrapolated the original cubes in order to accommodate the acquisition geometry. We simulated synthetic seismic shots for each model using a finite-difference wave propagator, isotropic, acoustic, with second-order in time, eight-order in space, and exponential attenuation on the absorbing boundaries. The acquisition geometry defines 4800 shots, with 50 meters of increment in inline and crossline directions. The simulated receivers are ten streamers 2000m long, spread with a maximum lateral distance of 500m from the source.

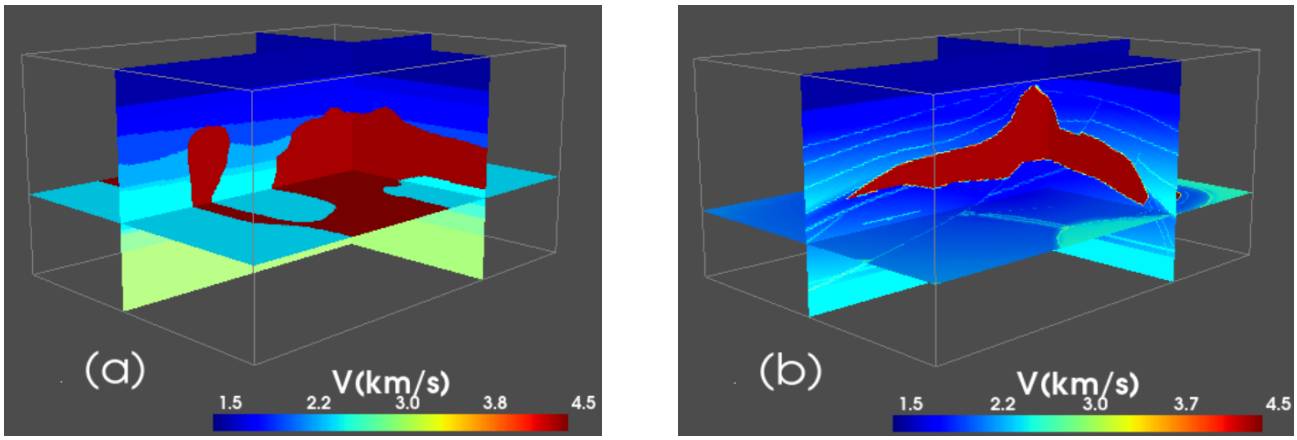

Figure 2: (a) shows one example of model from the training set, and (b) the SEG/EAGE salt model used to validate the generalization ability of the network.

We constructed the 3D velocity models using real salt geometries from velocity models built with tomography and FWI in regions with complex salt structures and high exploration interest in the past decade. To increase the complexity and diversity of the training set, we applied over those geometries a 3D augmentation algorithm [8], which rotates, flips, and resizes the original salt geometries. After the augmentation process, we resized the salt geometry to fit into the desired size and included it on a simple sediment velocity background. Figure 2(a) shows one example of the 30 generated models. Another velocity model used in the study was the SEG/EAGE 3D salt model [9], which is plotted in Figure 2(b).

We used a U-Net [10] as our network architecture of choice; it is composed of a contracting and a symmetric expanding path, defining a u-shape form. Each step in the contracting path consists of a series of convolutions followed by a pooling layer. The number of convolutional filters increases at each step and the spatial size decreases due to pooling. The expanding path does the opposite, using up-convolutions to upsample the image but reducing the number of filters at each step. During the expanding path, information from the contracting phase is concatenated to localize finer features better. The proposed architecture uses 3D convolutional blocks that were previously used for 3D interpretative geophysical tasks, e.g. [11]. The U-net architecture defines a flow in which the output image has the same size as the output, except for the number of channels. This feature is extremely convenient to our problem since migrated images and salt masks share the same dimensions except for the number of subsurface offsets, treated as channels of the input images.

The use of 3D convolutional blocks requires much memory and presents a longer training time when compared with 2D operations. In order to alleviate resource demands we subdivided the training models into smaller sections of 0.8km in depth, 1.2km in the crossline direction, and 1.6km in the inline direction, with respective steps of 0.4km, 0.6km, and 0.8km in each direction. This gives a total of 64 subcubes per model. During the training and validation phase, the subcubes were treated as independent. However, since the borders of the subcubes suffer from the lack of information from the neighborhood, we chose intentionally the division with superposition to combine the prediction results using a Hann windowing [12] to balance the results before summing the subcubes results. Since its a segmentation problem, we imposed the threshold of 0.5 to define salt and non-salt regions.

To train the U-Net we separated 28 models as validation/training sets, and left 2 models for testing. The network was trained for 80 epochs, using the Adam optimizer [13] with a learning rate of 0.0001, and the Jaccard loss[14]. We chose the weights when the validation loss was lowest as the best-trained U-Net to make the predictions for each sample in our test set. We divided the 3D models in the same way as in the training phase, this time keeping track of the origin of the subsets

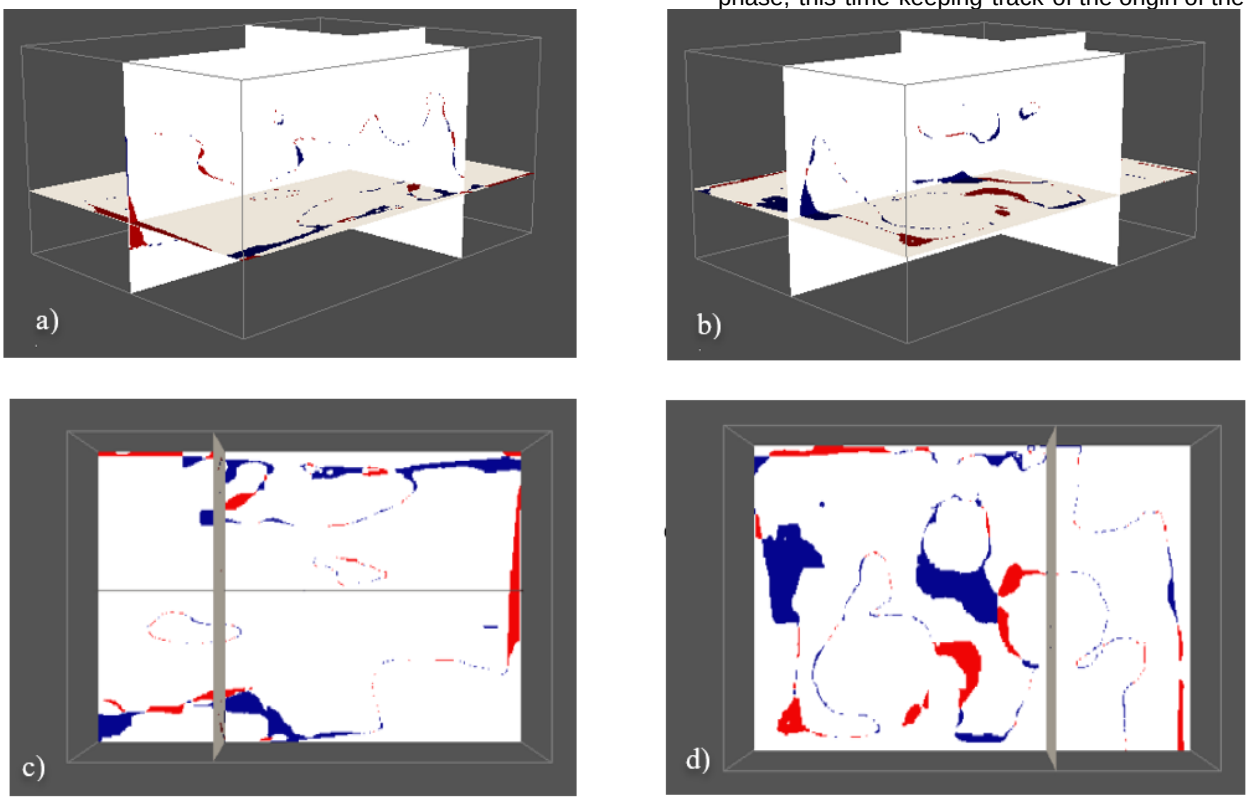

Figure 3: Difference between the predicted and the true salt mask. Figures (a) and (c) shows different angles from the same model, and (b) and (d) for another velocity model. Blue regions indicate false negative, and red false positive.

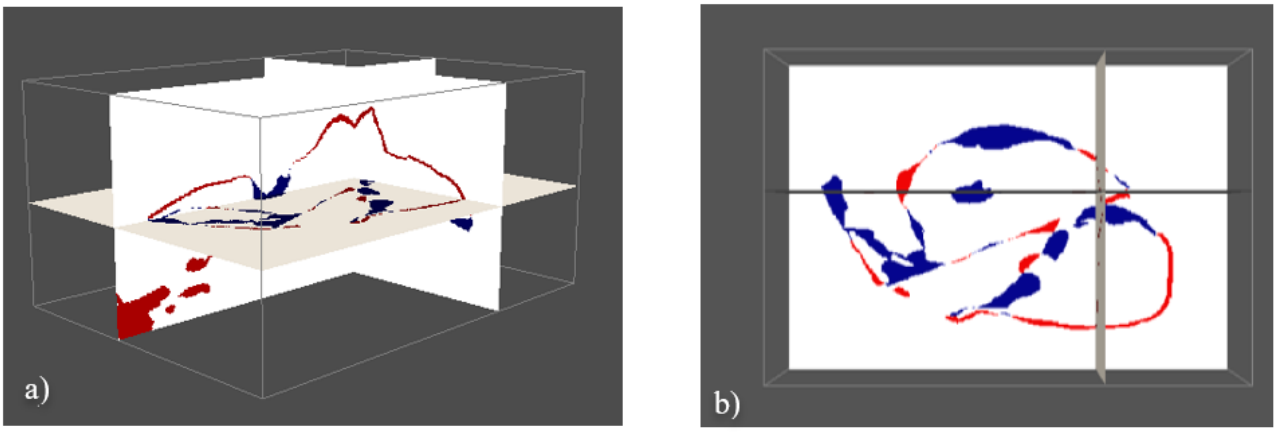

Figure 4: Difference between the predicted and the true salt mask for the SEG/EAGE salt model. Figures (a) and (b) shows different angles from the model. Blue regions indicate false negative, and red false positive.

to reassemble the salt models. When patching together the predictions, as previously mentioned, we used a Hann window in the areas of overlap between subsets.

Results

We evaluated the prediction accuracy of the trained U-Net over the two velocity models separated for test and also for the SEG/EAGE 3d salt model. It is worth mentioning that the SEG/EAGE salt model has its velocity values unaltered, being just rescaled to fit in the model dimensions investigated here.

Figure 3 shows the result for the models from the test set. It is possible to observe a great agreement between the true salt mask, and the predicted one. The similarity was also measured using the Dice similarity coefficient[15], suitable for imbalance class problems. The Dice Coefficient (DC) was equal to 0.94 for the model presented in Figure 4(a)(c), and equal to 0.9 for the model presented in Figure 4(b)(d).

Figure 4 shows the result for the SEG/EAGE 3D salt model, where it is possible to observe that the accuracy of prediction decays when compared with the test set. It is possible to observe a false positive region in the border of the model, and in general worse salt limits. The observed Dice Coefficient was equal to 0.64. Despite this score not being as good as the ones observed for the test set, this kind of model presents a challenge for the generalization

ability of the network, since the model velocity range and structures are completely different from the training set. It was previously shown in the 2D work [5] that the number and the distribution of the subsurface offset are important parameters to guarantee the same prediction score for the SEG/EAGE model. Different subsurface offset ranges and distributions were not yet investigated in the current work and are an open question.

Conclusions

Salt inclusion is particularly time-demanding over regions of allochthonous salt forming complex geometries, such as overhangs, teardrops and tongues. The method proposed here aims to solve the salt inclusion in one step with DL, reducing the time of the iterative process of salt flooding. Our results show that RTM migration using the sediment velocity generates subsurface offset gathers, which serve as the input for a DL model to identify the 3D true salt geometry, even for complex geometries.
We showed that it is possible to alleviate the memory demands of the 3D convolutional operators by dividing the migrated cubes into smaller ones. And that superposition and a suitable windowing are able to conciliate border effects. The predictions obtained present continuous salt geometries in both crossline and inline directions, with some mistakes in deep portions of the model.

This work is proof of the concept of salt segmentation over data migrated with 3D geometries and still requires further studies to be extended to real seismic data. In future studies, to improve the generalization ability of the method, the expansion of the number of volumes in the training data set must be investigated. And also the inclusion of more subsurface offset panels, probably with a cross variation of extended imaging condition lag in the x and y direction simultaneously.

To consider the application in real data, it will be necessary to expand the size of the volumes used for shot simulation and migration, increasing the depth of the interest geometries. Another improvement to make this technology viable for real data is to apply a matching filter between the wavelet used for synthetic data generation and the wavelet from real data.

Acknowledgements

APOM thanks Petrobras for sponsoring her postdoctoral research and for the permission to publish this work. JCC acknowledges the CNPq financial support through the INCT-GP and the grant 312078/2018-8 and Petrobras.

CRB acknowledges the financial support from CNPq (316072/2021-4) and FAPERJ (grants 201.456/2022 and 210.330/2022). Finally, the authors acknowledge the LITCOMP/COTEC/CBPF multi-GPU development team for supporting the Artificial Intelligence infrastructure and Sci-Mind's High-Performance multi-GPU system, and to SENAI CIMATEC Supercomputing Center for Industrial Innovation, for the cooperation, supply, and operation of computing facilities.

References

1. Dellinger, J., Brenders, A.J., Sandschaper, J.R., Regone, C., Etgen, J., Ahmed, I., Lee, K. J, 2017. The garden banks model experience. The Leading Edge, 36, 151–158.
2. Mousavi, S. M., Beroza, G. C., 2022, Deep-learning seismology. Science , 377, eabm4470.
3. Klatt, M., Faria, E.L., Muller, A.P.O., Coelho, J.M., González, J.L., de Albuquerque, M.P., Bom, C.R., Correia, M.D. [2022]. Deep learning strategy for salt model building, Geophysics 87, IM221-IM233.
4. Araya-Polo, M., S. Farris, and M. Florez, 2019, Deep learning-driven velocity model building workflow. The Leading Edge, 38, 872a1–872a9.
5. Muller, A.P.O., Costa, J.C., Bom, C.R., Faria, E.L., Klatt, M., Teixeira, G., de Albuquerque, M.P., 2022. Complete identification of complex salt geometries from inaccurate migrated subsurface offset gathers using deep learning, Geophysics 87, R453-R463.
6. AlAli, A., Kazei, V., Kalita, M. and Alkhalifah, T. [2022]. Deep learning unflooding for robust subsalt waveform inversion. Geophysical Prospecting.
7. Sava, P., and I. Vasconcelos, 2011, Extended imaging conditions for wave-equation migration. Geophysical Prospecting, 59, 35–55.
8. Solovyev, R., Kalinin, A.A., Gabruseva, T.[2022]. 3D convolutional neural networks for stalled brain capillary detection, Computers in Biology and Medicine 141, 105089.
9. Aminzadeh, F., Burkhard, N., Long, J. Kunz, T., Duclos, P.[1996]. Three dimensional seg/eaeg models - an update: The Leading Edge, 15, 131–134.
10. Ronneberger, O., P. Fischer, and T. Brox, 2015, U-net: Convolutional networks for biomedical image segmentation. Medical Image Computing and Computer-Assisted Intervention–MICCAI 2015, 234–241
11. Shi, Y., Wu, X., Fomel, S. [2019]. SaltSeg: Automatic 3D salt segmentation using a deep convolutional neural network, Interpretation 7, SE113-SE122.
12. Lizhe Tan, Jean Jiang, in Digital Signal Processing (Third Edition), 2019.
13. Kingma, D. P. and Ba, J. Adam: a method for stochastic optimization. 3rd International Conference on Learning Representations, ICLR 2015.
14. Duque-Arias, D., S. Velasco-Forero, J.-E. Deschaud, F. Goulette, A. Serna, E. Decencière, and B. Marcotegui, 2021, On power jaccard losses for semantic segmentation. VISAPP 2021: 16th International Conference on Computer Vision Theory and Applications.
15. Dice, Lee R., 1945. Measures of the Amount of Ecologic Association Between Species. Ecology. 26 (3): 297–302.